A Detailed Chemical Kinetic Model for the Supercritical Water Oxidation of Methylamine: The Importance of Imine Formation

A. M. Ashraful, Gabriel da Silva[1]

Department of Chemical Engineering, The University of Melbourne, Parkville 3010, Australia.

ABSTRACT

A detailed chemical kinetic model has been developed for supercritical water oxidation (SCWO) of methylamine, CH_3NH_2, providing insight into the intermediates and final products formed in this process as well as the dominant reaction pathways. The model was adapted from previous mechanisms, with a revision of the peroxyl radical chemistry to include imine formation, which has recently been identified as the dominant gas-phase pathway in amine oxidation. The developed model can reproduce previous experimental data on methylamine consumption and major product formation to reasonable accuracy, although with deficiencies in describing the induction time. Our simulations indicate that oxidation of the $^{\bullet}CH_2NH_2$ radical to methanimine, $CH_2{=}NH$, is the major channel in methylamine SCWO, with subsequent hydrolysis of $CH_2{=}NH$ providing the experimentally observed reaction products ammonia and formaldehyde. Integral-averaged reaction rates were used to identify major reaction pathways, and a first-order sensitivity analysis indicated that the concentration of CH_3NH_2 is most sensitive to OH radical kinetics. Overall, this work clarifies the importance of imine chemistry in the oxidation of nitrogen-containing compounds and indicates that they are necessary to model these compounds in SCWO processes.

Keywords: Supercritical water oxidation, chemical kinetic model, methylamine, imine

Introduction

Nitrogen-containing organic compounds are used widely throughout the chemical, petrochemical and pharmaceutical industries, and supercritical water oxidation (SCWO) is a potential means of destroying hazardous waste streams containing these chemicals.[1] Methylamine (CH_3NH_2) represents the simplest organic nitrogen compound, although there have been relatively few studies of its SCWO,[2,3] or of other more complicated nitrogen compounds.[4-10] Furthermore, although we have a relatively good understanding of the oxidation kinetics of small hydrocarbons,[11-13] oxygenated organics,[14-17] and ammonia[18-20] in

---

[1] Corresponding author: gdasilva@unimelb.edu.au

This is the author manuscript accepted for publication and has undergone full peer review but has not been through the copyediting, typesetting, pagination and proofreading process, which may lead to differences between this version and the Version of Record. Please cite this article as doi: 10.1002/kin.21393.

supercritical water, the detailed chemical kinetic models developed for methylamine SCWO by Benjamin and Savage[2] and by Li and Oshima[3] demonstrate several shortcomings. In particular, they can not accurately describe the formation and loss of the major nitrogen containing products and intermediates, such as NH_3, N_2O and N_2. In both models, the authors attributed this to deficiencies in the peroxyl radical chemistry, specifically the fate of the α-aminomethylperoxyl radical, $NH_2CH_2O_2^{\bullet}$.

It has been recently discovered that alkylperoxyl radicals with α-amino groups undergo facile $HO_2^{\bullet}$ elimination to produce imines (species with a C=N moiety).[21] In the prototypical methylamine case, the $^{\bullet}CH_2NH_2$ radical associates with O_2 to produce the $NH_2CH_2O_2^{\bullet}$ peroxyl radical intermediate, which loses $HO_2^{\bullet}$ to give methanimine, CH_2NH. Under atmospheric conditions, imine formation is now known to be the dominant fate for the oxidation of α-aminoalkyl radicals.[22] We were therefore motivated to update amine SCWO mechanisms to include imine chemistry. Moreover, imines are known to readily undergo hydrolysis in water.[23] In the case of methylamine SCWO, the imine product CH_2NH may, therefore, be able to react with H_2O to give ammonia (NH_3) and formaldehyde (HCHO). Ammonia is the primary nitrogen containing product of methylamine SCWO, whereas the dominant carbon bearing product is CO, which can readily form from formaldehyde. On this basis, in this study we have set out to update and validate a detailed chemical kinetic model for the oxidation of methylamine in supercritical water oxidation that includes imine chemistry.

Kinetic Modelling

Model Development

The detailed chemical kinetic model (DCKM) employed here was constructed based on the prior models of Benjamin and Savage (referred to henceforth as the Benjamin or Bjm model) and of Li and Oshima (the Li model), which themselves built upon earlier SCWO models for alcohols and gas-phase combustion mechanisms for methylamine. Our model consists of all reactions and rate parameters from the Benjamin model, with additional amine reactions included from the work Li and Oshima (indicated in the Supporting Information). Both the Benjamin and Li models included different $NH_2CH_2O_2^{\bullet}$ peroxyl radical chemistry, as shown in Figure 1, and predate the finding that these peroxyl radicals preferentially decompose to yield imines.[21] Imines are well-known to undergo hydrolysis to amines and carbonyls via acid-base chemistry.[24]

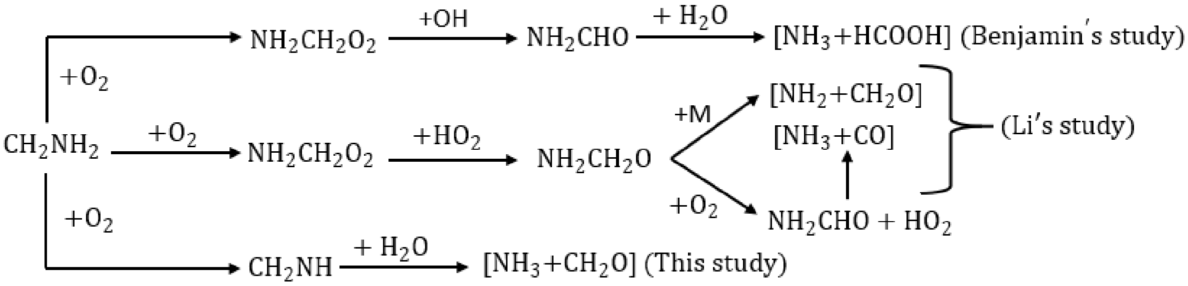

Figure 1: Peroxyl radical mechanisms employed in prior methylamine models (Benjamin and Li) and in this study.

Hayashi et al.[17] recently presented an up-to-date kinetic model for SCWO of methanol and ethanol, which we adopted as the H,C,O chemistry set for our model. On top of this, the required chemical reactions involving nitrogen-containing species were adopted from Li's[3] and Benjamin's[2] studies. We adopted the formamide thermal dissociation reactions[25] as well as water-assisted reactions from the Benjamin model.[2] Given the ability for acid-base reactions to proceed in supercritical water,[13] we also incorporated hydrolysis of CH_2NH to produce formaldehyde (CH_2O) and ammonia (NH_3), as detailed below. The complete kinetic model is provided in the Supporting Information.

Initial H abstraction from methylamine (CH_3NH_2) by hydroxyl ($^\bullet OH$) radical in the gas phase proceeds via two significant reaction routes (R341 and R344):

$$\mathrm{CH_3NH_2 + OH \rightarrow CH_2NH_2 + H_2O} \qquad \text{R341}$$

$$\mathrm{CH_3NH_2 + OH \rightarrow CH_3NH + H_2O} \qquad \text{R344}$$

Experimentally, the total rate coefficient for CH_3NH_2 + OH has been determined to be around 10×10^{12} cm^3 mol^{-1} s^{-1} at temperatures of *ca.* 300 – 400 K. [26,27] This value suggests a near-barrierless process, which is supported by theoretical studies.[28,29] The temperature dependence and branching fractions for the CH_3NH_2 + OH reaction remains somewhat unclear.

Kinetic modelling of methylamine oxidation in a shocktube at 1260 – 1600 K fit a total CH_3NH_2 + OH rate coefficient of *ca*. 3×10^{12} – 6×10^{12} cm^3 mol^{-1} s^{-1}.[30] A theoretical study by Tian *et al*.[29] predicted *k* values of around 20×10^{12} cm^3 mol^{-1} s^{-1} at between 300 – 1000 K, in relatively good agreement with the room temperature experiments, and suggesting that the reaction is not very sensitive to temperature under the conditions relevant to our study. At higher temperatures the rate coefficient is predicted to increase somewhat, yielding predictions that are around a factor of 2 to 3 above the shocktube values. It is therefore not obvious if the reaction should be treated with a small positive or negative activation energy, although all available evidence indicates that the rate coefficient will not deviate significantly from the accurately measured room temperature values across the range of temperatures studied here, and we have therefore set the total rate coefficient to a constant value of 10×10^{12} cm^3 mol^{-1} s^{-1}.

There is even less information available for the CH_3NH_2 + OH branching fractions, although C—H abstraction is typically favoured over N—H abstraction in amines,[31] and the experimental studies assumed CH_2NH_2 to be the major reaction product. The Tian *et al*.[29] study predicted branching of around 70 – 80 % toward CH_2NH_2, whereas a separate theoretical study by Galano and Alvarez-Idaboy [28] predicted a value of 80 %. We have adopted the latter recommendation, and therefore set k_{R341} as 8.0×10^{12} cm^3 mol^{-1} s^{-1} and k_{R344} as 2.0×10^{12} cm^3 mol^{-1} s^{-1}.

In this study, the subsequent oxidation of the aminomethyl radical ($^{\bullet}CH_2NH_2$) in supercritical water is assumed to proceed to methanimine (CH_2NH) and $HO_2^{\bullet}$, as occurs in the gas-phase at room temperature:

$$\mathrm{CH_2NH_2 + O_2 \rightarrow CH_2NH + HO_2} \qquad \text{R357}$$

The rate coefficient of reaction R357 has been estimated as k_{R357}=2.1×10^{13} cm^3 mol^{-1} s^{-1}, a typical value for alkyl radical association with O_2.

For the $CH_3N^{\bullet}H$ radical, our recent work[32] showed that it also undergoes a H-abstraction reaction with O_2 resulting in imine formation:

$$\mathrm{CH_3NH + O_2 \rightarrow CH_2NH + HO_2} \qquad \text{R371}$$

The rate coefficient of reaction R371 was calculated to be k_{R371} = 3.6×10^{-17} cm^3 $molecule^{-1}$ s^{-1}.[32]

The hydrolysis of imines in aqueous solution results in a carbonyl and an amine, following a retro-Schiff reaction.[24] If this would be the fate of CH_2NH, then NH_3 and CH_2O would be the hydrolysis products. Hence, reaction R358 is incorporated into our mechanism, with k_{R358}=1.0×10^{12} cm^3 mol^{-1} s^{-1}.

$$\mathrm{CH_2NH + H_2O \rightarrow CH_2O + \ NH_3} \qquad \text{R358}$$

Oxidation of CO to CO_2 is largely controlled by the CO + HNO reaction (the reverse of R266). The Benjamin model uses an estimate for this important rate coefficient, which is significantly faster than the experimental value of k_{R266}=1.0×10^{13} cm^3 mol^{-1} s^{-1} reported by Rohrig and Wagner.[33] Our model incorporates the latter value, which results in more accurate predictions of CO_2 yields (*vide infra*).

$$\mathrm{NH + CO_2 \rightarrow HNO + \ CO} \qquad \text{R266}$$

Reactor Simulations

To calculate the concentration of major products during the SCWO oxidation of methylamine we used the CHEMKIN-Pro-19.0 simulation software.[34] Simulations were performed at constant pressure under conditions representative of the experiments reported by Benjamin and Savage[2] and by Li and Oshima.[3] In the Li experiments the water concentration is not specified, and we estimated them from the stated temperature, pressure, and concentrations of methylamine and O_2 on an ideal gas basis. A maximum absolute tolerance of 1.0×10^{-15} was imposed to determine convergence.

Reactor simulations were interpreted with the aid of integratal averaged reaction rate and normalised sensitivity coefficients. The integratal averaged reaction rate, $\overline{R}_i$, for reaction *i* is given as:

$$\boldsymbol{\overline{R}_i = \frac{\int_0^{r} R_{i[net]}\,dt}{\tau}}$$

Where $R_{i[net]}\,dt$ is the net rate of reaction *i* and τ is the total residence time. The normalized sensitivity coefficient S_{ij}, for species *i* with respect to reaction *j*, was calculated based on the following expression:

$$\boldsymbol{S_{ij} = \frac{\partial \ln x_i}{\partial \ln k_j}}$$

Where x_i is the mole fraction of species *i* and k_j is the rate coefficient of reaction *j*.

Results & Discussion

The experimental and model-predicted methylamine concentrations during SCW oxidation in the experiments of Benjamin[2] and of Li[3] are depicted in Figure 2 and Figure 3, respectively. All experiments were conducted between 390 °C and 500 °C with excess O_2.

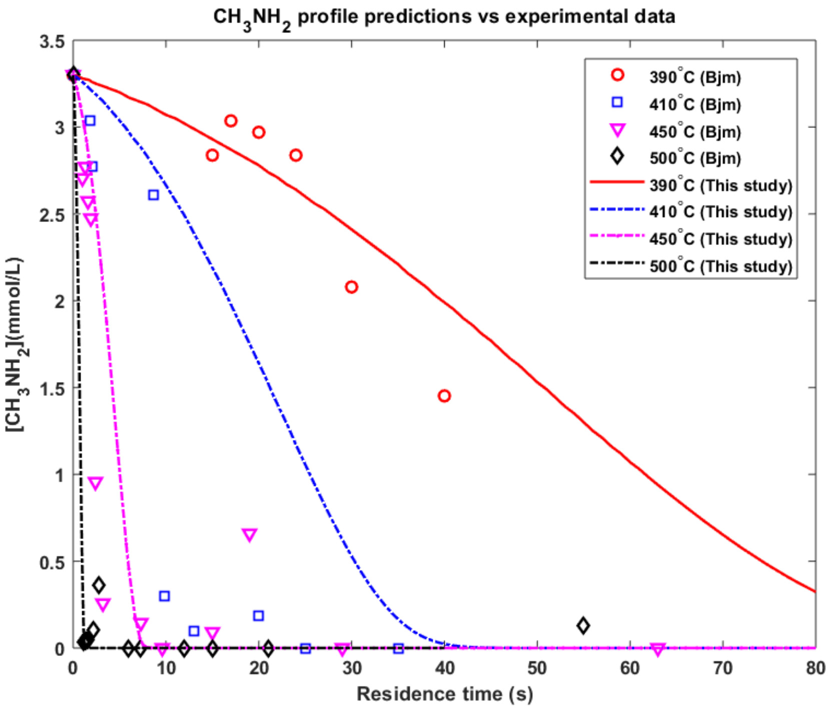

Figure 2. Experimental and simulated methylamine concentrations as a function of time and temperature, at a pressure of 249 atm under the experimental conditions of Benjamin and Savage. Initial concentrations: $[CH_3NH_2]_0$ = 3.31 mmole/L, $[O_2]_0$ = 17.9 mmole/L.

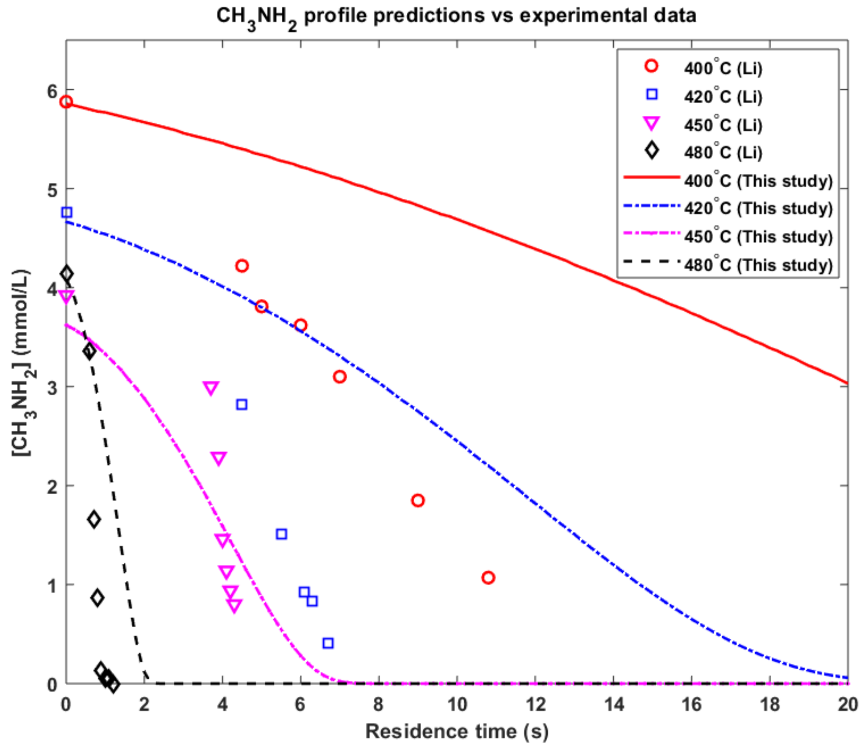

Figure 3. Experimental and simulated methylamine concentrations as a function of time and temperature, at a pressure of 247 atm under the experimental conditions of Li and Oshima. Initial concentrations: **(400 °C)** $[CH_3NH_2]_0$ = 5.9 mmole/L, $[O_2]_0$ =32.9 mmole/L. **(420 °C)** $[CH_3NH_2]_0$ = 4.8 mmole/L, $[O_2]_0$ =26.6 mmole/L. **(450 °C)** $[CH_3NH_2]_0$ = 3.9 mmole/L, $[O_2]_0$ =22 mmole/L. **(480 °C)** $[CH_3NH_2]_0$ = 4.1 mmole/L, $[O_2]_0$ =21.9 mmole/L.

Figure 2 demonstrates that the model results provide a relatively good description of both the induction period and methylamine disappearance rates observed in the experiments of Benjamin. For the simulations of Li's experiments, shown in Figure 3, we find that consistent agreement is only found at the highest temperatures (450 - 480 °C). At lower temperatures the rate of methylamine consumption is relatively well-described, although the induction period is substantially over-predicted. The induction period occurs due to the time-lapse of radical pool formation and inhomogeneous mixing in the fuel stream,[2] and is sensitive to the reactor material which can act as both a sink and source of free radicals. The inconsistency with reproducing the induction period, and the significant variation in induction period between the two sets of experiments performed under similar conditions, suggests that it is related to reactor wall chemistry, although we can not discount that it is due to deficiencies in modelling the HO_x radical chemistry.[12,35,36] Note also that residence times are considerably shorter in the Li experiments *vs*. those of Benjamin, and that errors in predicting the induction period for the former therefore appear amplified.

We now turn our attention to the predicted profiles of the product species measured in the methylamine SCWO experiments, *vis.*, NH_3, CO, and CO_2, which are plotted in Figures 4 and 5. In all experiments the intial co-evolution of NH_3 and CO as the major oxidation products is captured by our DCKM. Following the consumption of methylamine, the subsequent slower oxidation of ammonia and CO is described relatively accurately.

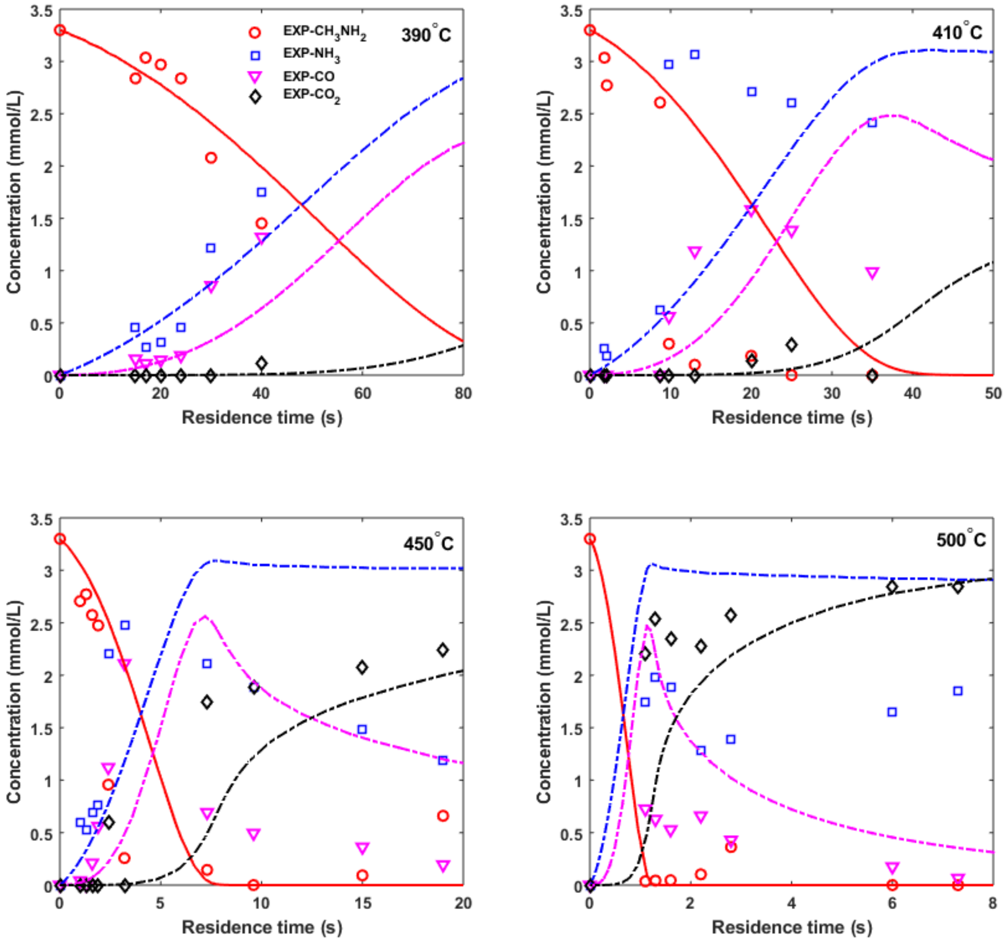

Figure 4. Comparison of products yields measured (symbols) for the experiments of Benjamin and simulated (dashed lines) for this study. Conditions as per Figure 2

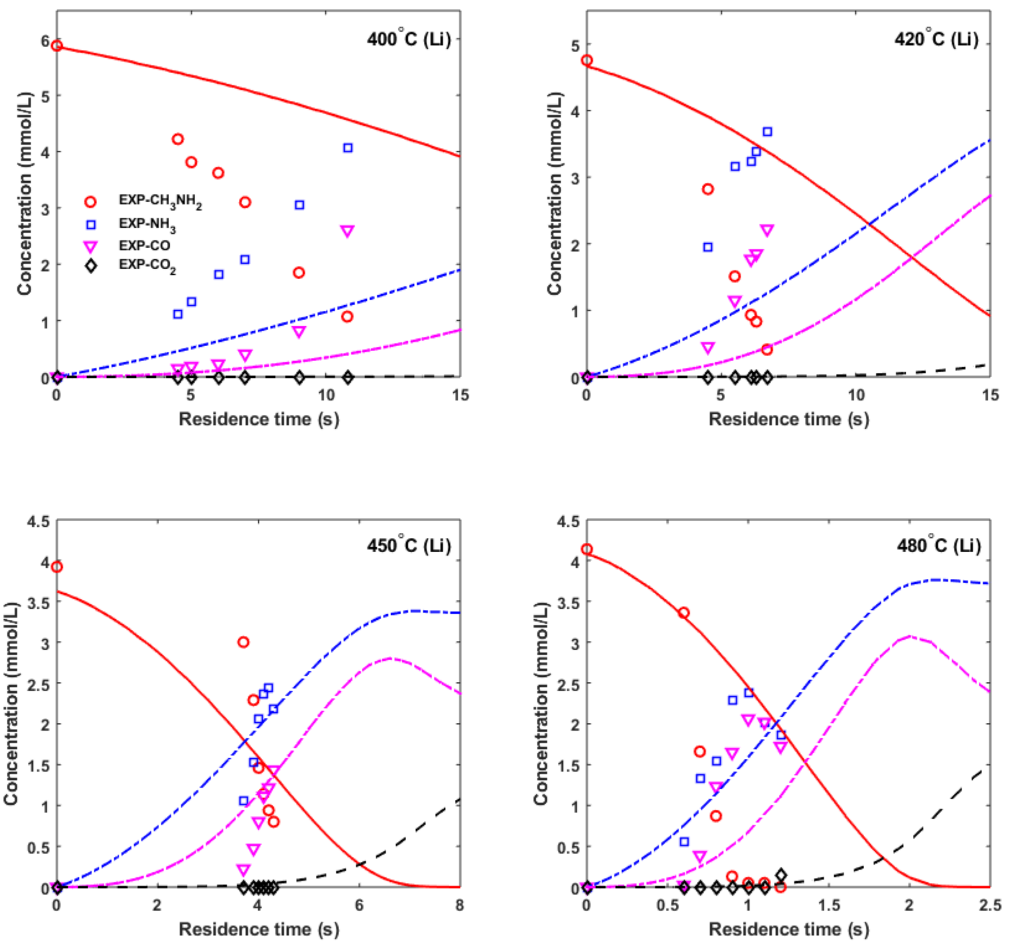

Figure 5. Comparison of products yields measured (symbols) for the experiments of Li and simulated (dashed lines) for this study. Conditions as per Figure 3.

Comparisons between the performance of the newly developed DCKM and the previous models is made in Figures A1 and A2 of the supporting material, for the key species NH_3 and CO_2. We find that our new model provides an improved description of ammonia formation, which was typically underpredicted in the previous studies. The oxidation of CO to CO_2 is also more accurately captured.

As mentioned, heterogeneous catalytic reactions at the reactor walls may be a cause of significant discrepancy between the experimental and modelled results, both during the establishment of the radical pool and during the fuel-lean later stages of reaction. Indeed, Benjamin and Savage[2] suspected that heterogeneous processes were playing a role in their experiments, because of the Hastelloy C-276 (57 % Ni) steel that their reactor was constructed from. It is well known that nickel and nickel-containing materials can influence the oxidation process of nitrogen-containing compounds .[37,38] In addition, a significant amount of hydrogen peroxide (H_2O_2) is predicted to accumulate during these experiments, which can also react catalytically at metal surfaces.

To further examine the important elementary reactions in methylamine SCWO, reaction path diagrams have been constructed on the basis of integral averaged reaction rates. The reaction path diagram and the integral averaged reaction rates are shown in Figures 6 and 7, respectively, with the absolute rate of production of the major species shown in Figures A3 - A6 (Supporting Information). The reaction path diagram only includes reactions with integral averaged rates of magnitude 10^{-6} or greater.

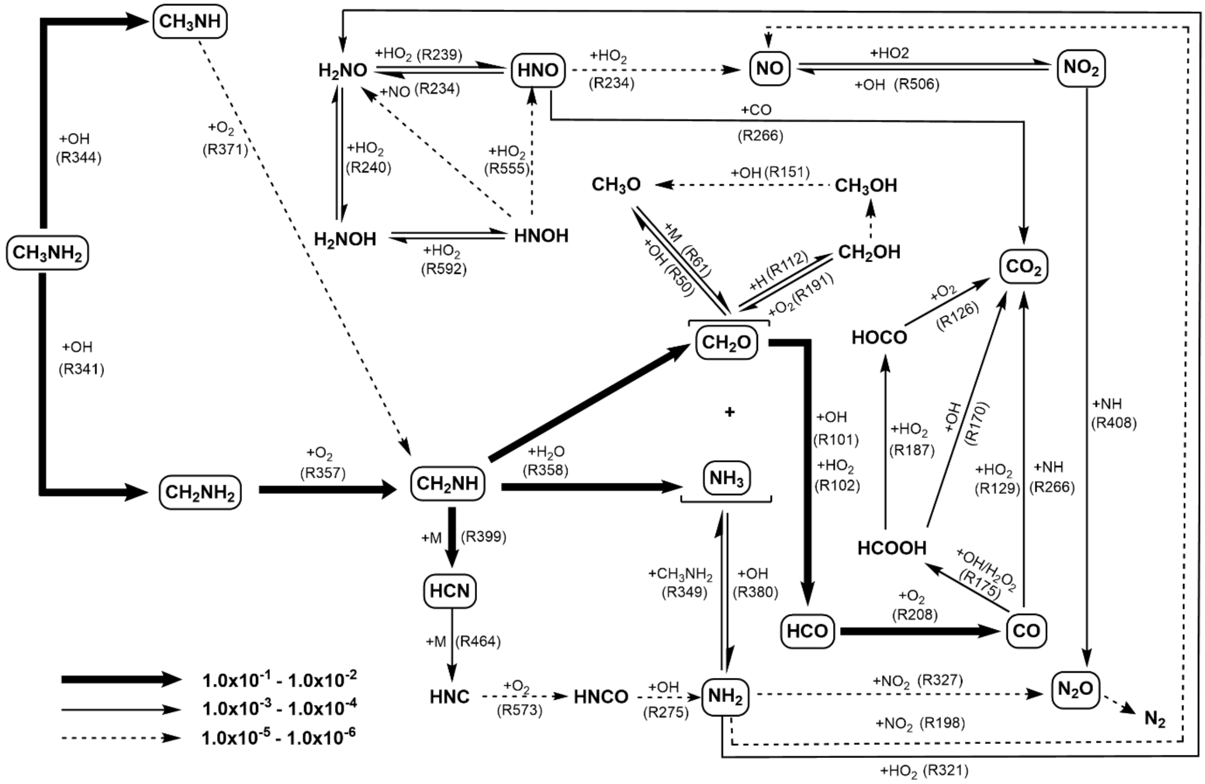

Figure 6: Major reaction paths during methylamine SCWO. Condition: 450 °C, 249 atm, *t* = 3 s, $[CH_3NH_2]$ = 3.31 mmol/L, $[O_2]$ = 17.9 mmol/L, $[H_2O]$ = 4190 mmol/L, and conversion = 0.32, Thickness of arrows indicates relative rate of each step.

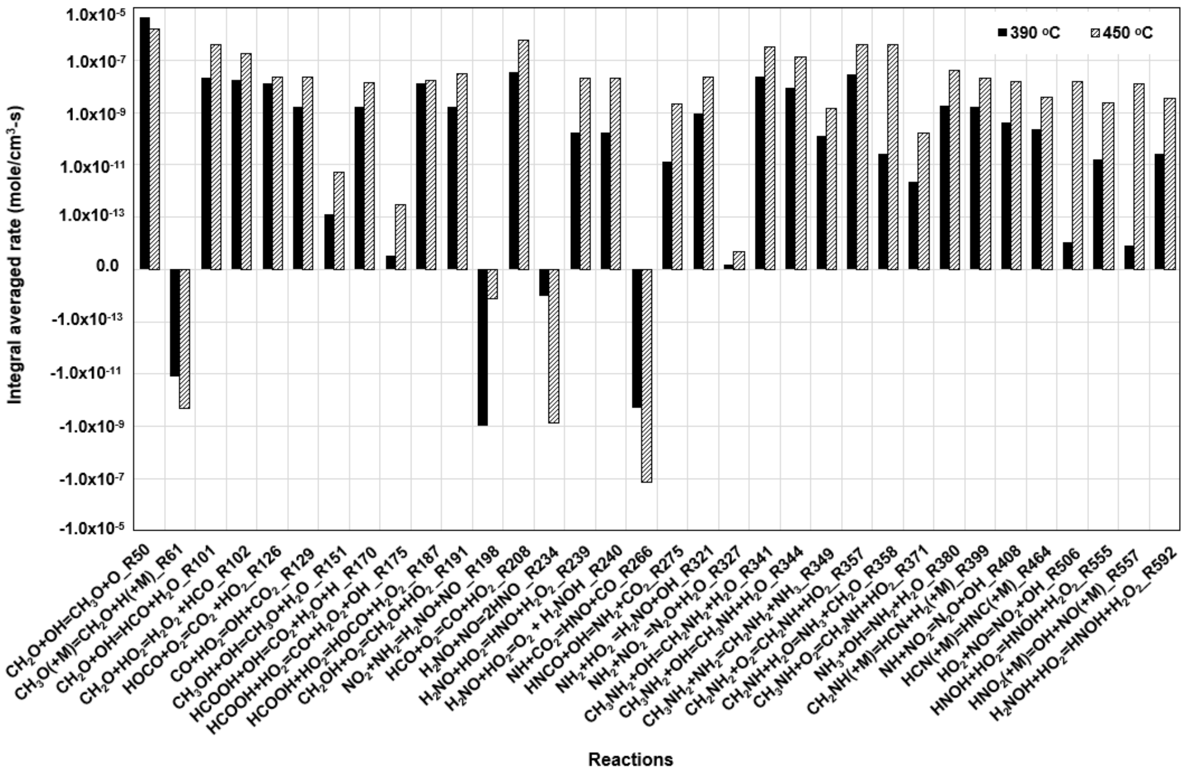

Figure 7: Integral averaged reaction rate comparisons between 390 °C and 450 °C. Condition: $[CH_3NH_2]$ = 3.31 mmol/L, $[O_2]$ = 17.9 mmol/L, $[H_2O]$ = 4190 mmol/L, and conversion = 0.32

The reaction path diagram shows that methylamine oxidation is primarily initiated by H abstraction by OH radical, at C and N sites to produce $^{\bullet}CH_2NH_2$ and $CH_3N^{\bullet}H$ (with H_2O) via reactions R341 and R344:

$$\mathrm{CH_3NH_2 + OH = CH_2NH_2 + \ H_2O} \qquad \text{R341}$$

$$\mathrm{CH_3NH_2 + OH = CH_3NH + \ H_2O} \qquad \text{R344}$$

Integral averaged reaction rates show that C—H abstraction is slightly preferred over N—H abstraction. Moreover, the absolute rate of production (Figure A3 and Figure A4) of $^{\bullet}CH_2NH_2$

and $CH_3N^{\bullet}H$ also supports reaction R341 as the dominant reaction process. Reaction R341 contributes more than 70 % of methylamine conversion to produce $^{\bullet}CH_2NH_2$, while only 17 % of methylamine consumed in the formation of $CH_3N^{\bullet}H$ is via reaction R344.

The major initial rection intermediate, $^{\bullet}CH_2NH_2$, reacts rapidly with O_2 to produce CH_2NH via reaction R357. The minor CH_3NH intermediate reaction with O_2 also leads to CH_2NH (R371), although with a higher barrier than the aminoalkyl radical case.

$$\mathrm{CH_2NH_2 + O_2 = CH_2NH + HO_2} \qquad \text{R357}$$

$$\mathrm{CH_3NH + O_2 = CH_2NH + HO_2} \qquad \text{R371}$$

The imine CH_2NH is the most significant first-generation closed-shell oxidation product of CH_3NH_2, and its further reactions therefore largely dictate the product distribution observed in methylamine SCWO. The absolute rate of production and integral averaged reaction rate analysis shows that hydrolysis is the domiant loss pathway for CH_2NH, producing NH_3 and CH_2O (R358):

$$\mathrm{CH_2NH + H_2O = NH_3 + \ CH_2O} \qquad \text{R358}$$

Alternatively, CH_2NH dissociation can proceed via successive H-abstraction reactions leading to the formation of HCN, which rapidly equilibriates with HNC and is then oxidised to HNCO through reactions R464 and R573. HNCO rapidly feeds into the amine pool, forming NH_2 via reaction R275.

$$\mathrm{HCN(+M) = HNC(+M)} \qquad \text{R464}$$

$$\mathrm{HNC + O_2 = HNCO + O} \qquad \text{R573}$$

$$\mathrm{HNCO + OH = NH_2 + \ CO} \qquad \text{R275}$$

The carbon-bearing product of imine hydrolysis, CH_2O, follows conventional H/C/O chemistry to form CO and CO_2. Another important contributor is the reaction of CO with HNO (the reverse of reaction R266).

$$\mathrm{NH + CO_2 = HNO + CO} \qquad \text{R266}$$

Ammonia has been experimentally identified as the major nitrogen-containing oxidation product of methylamine in supercritical water, and it is apparent that an accurate depiction of imine chemistry is required to reproduce this observation. The SCWO chemistry of ammonia is well understood, and being significantly less reactive than methylamine it accumulates to high levels in these experiments. We predict that the dominant removal channels for NH_3 are through N—H abstraction to OH radicals (R380), giving the aminyl radical NH_2. The subsequent reactions of NH_2 either lead to N_2O and then N_2 (N—N recombination reactions) or to NO and NO_2 (oxidation) via the reactions R327, R198 and R506.

$$\mathrm{NO_2 + NH_2 = H_2NO + NO} \qquad \text{R198}$$

$$\mathrm{NH_2 + NO_2 = N_2O + H_2O} \qquad \text{R327}$$

$$\mathrm{NH_3 + OH = NH_2 + H_2O} \qquad \text{R380}$$

$$\mathrm{HO_2 + NO = NO_2 + OH} \qquad \text{R506}$$

A sensitivity analysis was conducted to gain further insight into the sources and sinks of CH_2NH (Figure 8) and NO (Figure 9). For CH_2NH, the key reactions were found to be:

$$\mathrm{2HO_2 = H_2O_2 + O_2} \qquad \text{R15}$$

$$\mathrm{H_2O_2(+M) = 2OH(+M)} \qquad \text{R19}$$

$$\mathrm{H_2O_2 + OH = H_2O + HO_2} \qquad \text{R20}$$

$$\mathrm{CH_2O + HO_2 = H_2O_2 + HCO} \qquad \text{R102}$$

$$CH_3NH_2 + OH = CH_2NH_2 + H_2O \qquad R341$$

$$CH_3NH_2 + OH = CH_3NH + H_2O \qquad R344$$

$$CH_3NH_2 + O_2 = CH_2NH_2 + HO_2 \qquad R352$$

$$CH_2NH_2 + H_2O_2 = CH_3NH_2 + HO_2 \qquad R359$$

$$CH_2NH(+M) = HCN+H_2\ (+M) \qquad R399$$

$$HCN\ (+M) = HNC\ (+M) \qquad R464$$

The most sensitive steps in the production and consumption of CH_2NH are simply those leading to OH radical production (*e.g.*, R15, R20), and the subsequent reaction of OH with CH_3NH_2 (R341, R344). Additionally, methylamine oxidation initiated by O_2 (R352) and HO_2 (R359) is also predicted to play a role. Interestingly, imine yields are insensitive to changes in rate coefficients for the major reactions directly leading to CH_2NH production ($^{\bullet}CH_2NH_2$ + O_2) and consumption (CH_2NH + H_2O) given their rapid reaction rates and lack of competing channels.

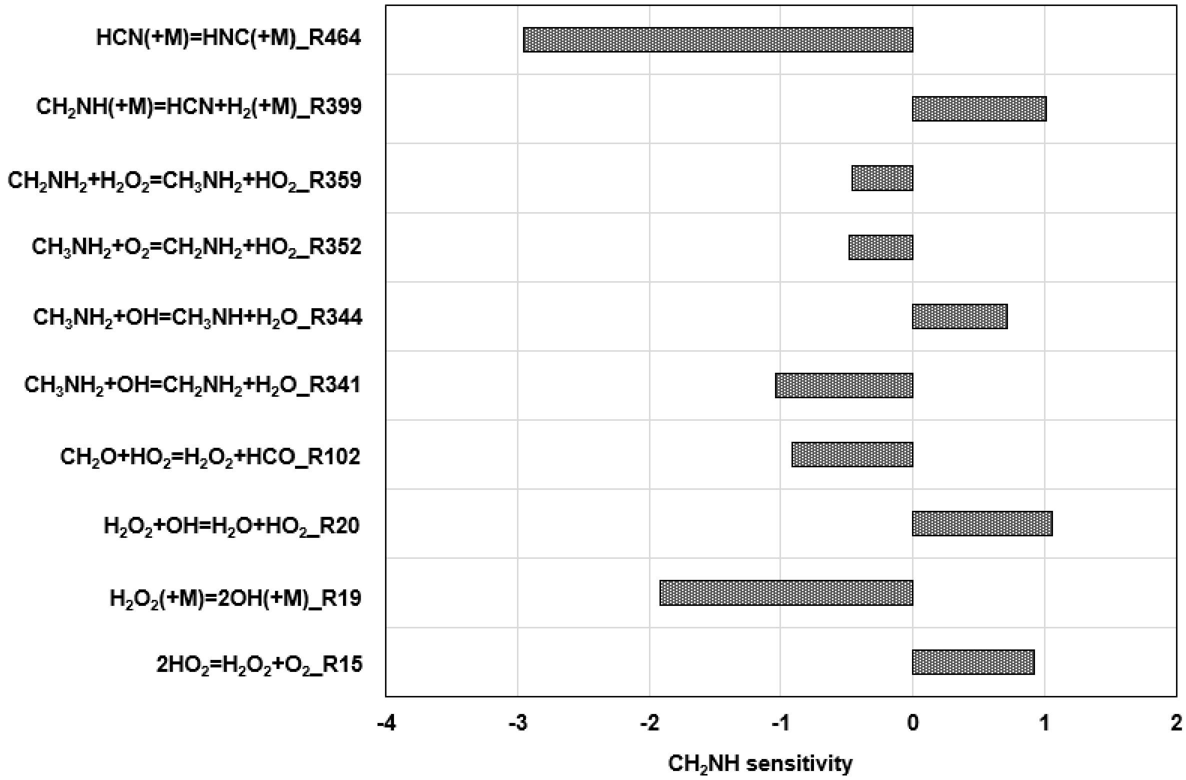

Figure 8: Normalized sensitivity coefficients for CH_2NH. Condition: 450 °C, 249 atm, $[CH_3NH_2]$ = 3.31 mmol/L, $[O_2]$ = 17.9 mmol/L, $[H_2O]$ = 4190 mmol/L.

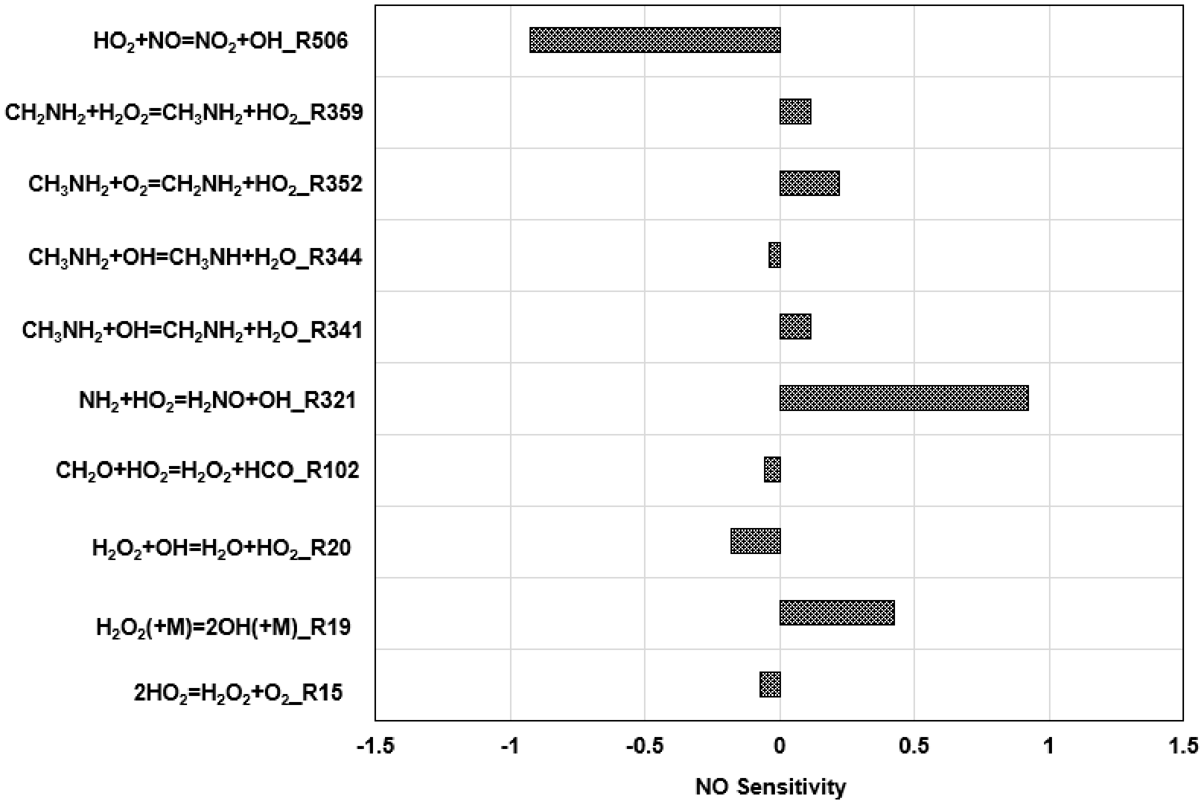

Figure 9: Normalized sensitivity coefficients for NO. Condition: 450 °C, 249 atm, $[CH_3NH_2]$ = 3.31 mmol/L, $[O_2]$ = 17.9 mmol/L, $[H_2O]$ = 4190 mmol/L.

Figure 9 represents NO sensitivity coefficients as a function of reaction temperature. In addition to many of the reactions discussed above responsible for establishing the radical pool and for initiating methylamine oxidation, The rate of CH_3NH radical formation via direct OH attack on CH_3NH_2 (R344) can play minor roles for NO consumption. According to the updated model, around two thirds of the NO yield is from HNO, where HNO is formed from H_2NO via reaction R239. Reaction R321 has positive sensitivity coefficents, indicating the importance to NO or N_2 formation of both direct routes from ammonia (NH_3 → NH_2 → NH) and other minor routes (e.g. HCN → HNC → HNCO → NH_2).

$$NH_2 + HO_2 = H_2NO + OH \qquad \text{R321}$$

Conclusions

We have developed an improved detailed chemical kinetic model for the supercritical water oxidation of methylamine. Through the inclusion of updated peroxyl radical chemistry this model can describe the efficient conversion of methylamine to ammonia which has been observed experimentally but was not accurately captured in previous models. This process proceeds via oxidation of the CH_2NH_2 radical to CH_2NH, followed by subsequent hydrolysis of this imine to produce CH_2O and NH_3. The description of CO_2 formation is also improved, primarily due to changes in the rate of the CO + HNO reaction. Remaining deficiencies in the model are largely attributed to heterogeneous wall chemistry, which causes discrepant induction times between the two sets of available experimental data, making further model improvements challenging.

Supporting Information Available: Kinetic model files.

References

1. Fang, Z.; Xu, C. C. Near-critical and supercritical water and their applications for biorefineries; Springer, 2014.
2. Benjamin, K. M.; Savage, P. E. Industrial & Engineering Chemistry Research 2005, 44, 5318-5324.
3. Li, H.; Oshima, Y. Industrial & Engineering Chemistry Research 2005, 44, 8756-8764.
4. Abraham, M. A.; Klein, M. T. Industrial & Engineering Chemistry Product Research and Development 1985, 24, 300-306.
5. Lee, D. S.; Gloyna, E. F. Environmental Science & Technology 1992, 26, 1587-1593.
6. Crain, N.; Tebbal, S.; Li, L.; Gloyna, E. F. Industrial & Engineering Chemistry Research 1993, 32, 2259-2268.
7. Lee, D. S.; Do Park, S. Journal of Hazardous Materials 1996, 51, 67-76.
8. Lee, D. S.; Park, K. S.; Nam, Y. W.; Kim, Y.-C.; Lee, C. H. Journal of Hazardous Materials 1997, 56, 247-256.
9. Funazukuri, T.; Takahashi, M. Fuel 1999, 78, 1117-1119.
10. Aymonier, C.; Beslin, P.; Jolivalt, C.; Cansell, F. The Journal of Supercritical Fluids 2000, 17, 45-54.
11. Brock, E. E.; Savage, P. E. AIChE Journal 1995, 41, 1874-1888.
12. Savage, P. E.; Yu, J.; Stylski, N.; Brock, E. E. The Journal of Supercritical Fluids 1998, 12, 141-153.

13. Savage, P. E. Chemical Reviews 1999, 99, 603-622.
14. Webley, P. A.; Tester, J. W.; ACS Publications, 1989.
15. Brock, E. E.; Oshima, Y.; Savage, P. E.; Barker, J. R. The Journal of Physical Chemistry 1996, 100, 15834-15842.
16. Rice, S. F.; Croiset, E. Industrial & Engineering Chemistry Research 2001, 40, 86-93.
17. Hayashi, R.; Onishi, M.; Sugiyama, M.; Koda, S.; Oshima, Y. The Journal of Supercritical Fluids 2007, 40, 74-83.
18. Webley, P. A.; Tester, J. W.; Holgate, H. R. Industrial & Engineering Chemistry Research 1991, 30, 1745-1754.
19. Ploeger, J. M.; Green, W. H.; Tester, J. W. International Journal of Chemical Kinetics 2008, 40, 653-662.
20. Shimoda, E.; Fujii, T.; Hayashi, R.; Oshima, Y. The Journal of Supercritical Fluids 2016, 116, 232-238.
21. da Silva, G.; Kirk, B. B.; Lloyd, C.; Trevitt, A. J.; Blanksby, S. J. The Journal of Physical Chemistry Letters 2012, 3, 805-811.
22. Rissanen, M. P.; Eskola, A. J.; Nguyen, T. L.; Barker, J. R.; Liu, J.; Liu, J.; Halme, E.; Timonen, R. S. Journal of Physical Chemistry A 2014, 118, 2176-2186.
23. Ciaccia, M.; Di Stefano, S. Organic & Biomolecular Chemistry 2015, 13, 646-654.
24. Layer, R. W. Chemical Reviews 1963, 63, 489-510.
25. Ferus, M.; Michalčíková, R.; Shestivská, V.; Šponer, J. í.; Šponer, J. E.; Civiš, S. Journal of Physical Chemistry A 2014, 118, 719-736.
26. Carl, S.; Crowley, J. Journal of Physical Chemistry A 1998, 102, 8131-8141.
27. Atkinson, R.; Perry, R.; Pitts Jr, J. Journal of Chemical Physics 1977, 66, 1578-1581.
28. Galano, A.; Alvarez-Idaboy, J. R. Journal of Chemical Theory and Computation 2008, 4, 322-327.
29. Tian, W.; Wang, W.; Zhang, Y.; Wang, W. International Journal of Quantum Chemistry 2009, 109, 1566-1575.
30. Hwang, S.; Higashihara, T.; Gardiner, W.; Shin, K. Journal of Physical Chemistry 1990, 94, 2883-2889.
31. Borduas, N.; Abbatt, J. P.; Murphy, J. G.; So, S.; da Silva, G. Environmental Science & Technology 2016, 50, 11723-11734.
32. Alam, M. A.; Ren, Z.; da Silva, G. International Journal of Chemical Kinetics 2019.
33. Röhrig, M.; Wagner, H. G. Symposium (International) on Combustion, 1994, pp 975-981.
34. CHEMKIN, P. Inc.: San Diego 2018.
35. Hochgreb, S.; Dryer, F. Combustion and Flame 1992, 91, 257-284.
36. Minetti, R.; Ribaucour, M.; Carlier, M.; Fittschen, C.; Sochet, L. Combustion and Flame 1994, 96, 201-211.
37. Schoofs, G. R.; Benziger, J. B. Journal of Physical Chemistry 1988, 92, 741-750.
38. Chang, C. C.; Khong, C.; Saiki, R. Journal of Vacuum Science & Technology A: Vacuum, Surfaces, and Films 1993, 11, 2122-2127.